Interaction between Magnetic Order and the Vortex Lattice in $HoNi_2B_2C$

C. D. Dewhurst,[1] R. A. Doyle,[2] E. Zeldov,[3] and D. McK. Paul[1]

[1]*Department of Physics, University of Warwick, Coventry CV4 7AL, United Kingdom*
[2]*Interdisciplinary Research Centre in Superconductivity, University of Cambridge, Cambridge CB3 0HE, United Kingdom*
[3]*Department of Condensed Matter Physics, The Weizmann Institute of Science, 76100 Rehovot, Israel*
(Received 24 July 1998)

Local Hall probe array magnetization measurements have been made on single crystals of the magnetic superconductor $HoNi_2B_2C$. Measured flux profiles show that surface barriers dominate the hysteresis below $T_c (\simeq 8.9K)$ except in a narrow temperature range between 5 and 5.75 K where superconductivity is strongly suppressed due to the onset of an *a*-axis incommensurate ordering of the Ho moments. The data presented show that the magnetic order also has a profound influence on the nonequilibrium (vortex-pinning) properties of the superconducting state.   [S0031-9007(98)08300-8]

Rare-earth nickel boro carbides [(RE)Ni$_2$B$_2$C] are an exciting class of materials offering the possibility of coexistence and interactions between superconducting and magnetically ordered states at low temperatures. The RE site may be occupied by both nonmagnetic Y and Lu ions, as well as magnetic Ho, Er, Tm, or Dy ions presenting systems with varying types of magnetic order coinciding with the superconducting state [1–6]. The superconducting transition temperatures, T_c, vary from about 15 K for RE = Y and Lu to 6 K for Dy, scaling roughly with the magnetic pair-breaking de Gennes factor for the RE ions indicating strong interactions between the isolated moments and superconducting electrons [4]. For RE = Ho, Er, and Tm, magnetic ordering occurs below T_c while for RE = Dy order is established above T_c. The magnetic order in these compounds is incommensurate in most cases, becoming antiferromagnetic and commensurate only with the underlying crystal structure at the lowest temperatures [5–7]. The occurrence of magnetic order within the superconducting state has provoked much interest in the detailed mechanisms of the coupling between magnetism and superconductivity [8].

Studies of the mixed state in the (RE)Ni$_2$B$_2$C materials have focused mainly on the structure of the vortex lattice (VL) as investigated by small angle neutron scattering (SANS) [9–12]. These measurements show the existence of a well-formed "clean" VL over much of the phase diagram indicating the absence of strong pinning effects. Field driven structural changes of the VL have been observed for RE = Er [9], Lu [10], Y [11], and Tm [12], high-lighting the dominance of nonlocal effects, in agreement with recent theoretical analysis [8]. More subtle changes in VL structure for the magnetic Er [9] and Tm [12] materials, on the other hand, appear to indicate that direct interactions with the localized moments may also be important. While flux pinning in the (RE)Ni$_2$B$_2$C materials is believed to be weak, few detailed experiments have attempted to examine the nature of possible effects of magnetic ordering on the pinning of vortices, despite its obvious fundamental interest.

In this Letter we report local Hall probe measurements of single crystals of $HoNi_2B_2C$, with $T_c = 8.9$ K, $B_{c2}(0) \simeq 8$ kG [6,13] and transition into a commensurate antiferromagnetic (AF) state at $T^m_{AF} \simeq 5$ K [3,5–7]. A schematic superconducting and magnetic phase diagram for $HoNi_2B_2C$ is shown in Fig. 1 [3,5–7,13]. The upper critical field has a nonmonotonic dependence on temperature with a clear reentrant behavior which begins just above T^m_{AF} [3,6,13]. Neutron scattering measurements of the nuclear and magnetic lattices show that the Ho moments lie in the *ab* plane and order differently in the three temperature regimes marked in Fig. 1 [5–7]. In region (*C*), below T^m_{AF}, the in-plane moments show AF order from plane to plane, commensurate with the crystal lattice in the *c* axis direction. Above T^m_{AF}, remnants of the ordered AF phase persist in the form of spiral modulations of the in-plane moments. These are incommensurate with
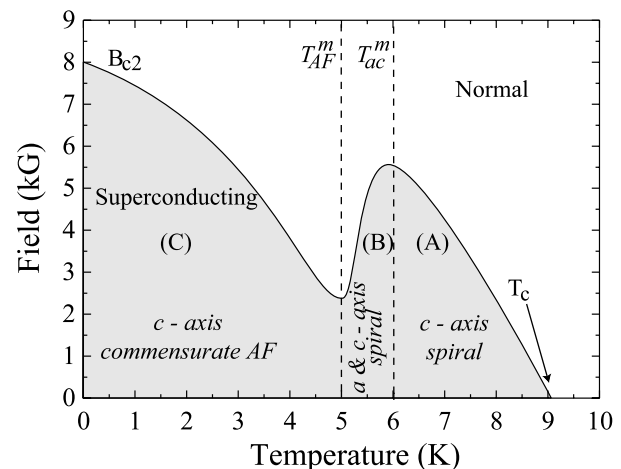

FIG. 1. Superconducting and magnetic phase diagram for $HoNi_2B_2C$. (*C*): Commensurate AF structure along the *c* axis (0 K to $T^m_{AF} \simeq 5$ K); (*B*): incommensurate spiral in the *c* and *a* axes (T^m_{AF} to $T^m_{ac} \simeq 6$ K); (*A*): incommensurate spiral structure in the *c* axis only (T^m_{ac} to $\simeq 9$ K) [5–7]. B_{c2} is reentrant around region (*B*) due to competition between the superconducting and magnetic order [3,6,13].

the crystal lattice in both the c- and a-axis directions in region (B) and c axis only in region (A). The a-axis spiral in region (B), between T_{AF}^m and T_{ac}^m, is thought to be responsible for the suppression of B_{c2} [3,6,7,13]. Here we probe the nonequilibrium properties of the vortices within the three temperature regimes. We show that the vortex lattice in HoNi$_2$B$_2$C is weakly pinned and dominated by surface barriers in regions (A) and (C), while in region (B) there is clear evidence for bulk pinning. We propose that the suppression of B_{c2} is insufficient to account for our observations and suggest that this is direct evidence for pinning of vortices by the ordered magnetic states.

Single crystals of HoNi$_2$B$_2$C were grown using a high-temperature flux method [14]. Regular shaped crystals were separated from the Ni$_2$B flux and cut into bars of dimensions 1 mm $\times$ 150 $\times$ 50 μm using a miniature wire saw. One of the optically smooth, as-prepared, crystal surfaces ($\perp c$) was positioned directly onto the GaAs/AlGaAs Hall array [15] of eleven sensors of active area of 10 $\times$ 10 μm and spacing of 10 μm. Eight sensors covered the width of the crystal [sensors 4–11: Fig. 2(a), inset] leaving three sensors to one side to measure the applied ($H\|c$) and demagnetizing fields (sensors 1–3).

Figure 2 shows representative *local* magnetization curves, $B_z - H_a$, as a function of applied field, H_a (left panel) with the corresponding field profiles measured by the Hall probe array (right panel). The data shown in Figs. 2(a)–2(c) at temperatures of 6.10, 5.37, and 3.60 K are representative of those collected in each of the regions (A), (B), and (C) of the phase diagram depicted in Fig. 1. Figure 2(a) shows local magnetization curves at a temperature of 6.10 K as determined by sensors 7 and 4 located at the center and edge of the crystal. The hysteretic magnetization shows pronounced asymmetry about the expected reversible magnetization, with a flat descending field leg and a small remanent magnetization. This is consistent with very weak bulk pinning and the dominance of surface [15–17] or geometrical barrier effects [15,18]. Comparison of the data determined at different locations across the sample shows that penetrating flux appears first at the sample center, at a field H_{p7}, and only later at the edge. Hysteresis is widest for the magnetization recorded at the sample edge rather than the center. This is opposite to what is expected for a critical state and consistent with both the surface or geometrical barrier [15,18]. The field profiles for increasing (open symbols) and decreasing (solid symbols) fields are shown in the right panel of Fig. 2(a). A large gradient in the local field between the outer (sensor 2) and inner (sensor 4) edge of the crystal in increasing field implies that large screening currents flow on the sample edge. The absence of significant bulk pinning means that vortices penetrating the surface or geometrical barrier at the edge are accelerated by the nonuniform demagnetizing field, forming a "flux pool" at the sample center and almost flux free regions close to the sample

edges [15,18]. In decreasing field the profile is modified dramatically and is almost flat with internal and external fields almost equal. This means that vortices exit freely as the field is reduced and is more consistent with a Bean-Livingston type of surface barrier [15–17] than a geometrical barrier scenario where the flux profile remains "domelike" in decreasing field due to finite edge currents which trap vortices in the sample. Finally, we note that the aspect ratio of the sample is only 3 so that the geometrical barrier is not expected to dominate the response [15,18].

Figure 2(b) shows magnetization loops measured in region (B) at 5.37 K. The magnitude of the loops is now reduced compared to (a) which might not be regarded as surprising since there is a clear minimum in B_{c2} in this temperature range [3,6,13]. On the other hand, the vortex solid phase is not in equilibrium and hysteresis determined by pinning need not necessarily show any correlation with B_{c2}. The hysteresis loops are now more symmetric, display a large remanent moment, and are widest for the magnetization recorded at the sample center. This suggests that surface barrier effects no longer dominate the vortex behavior at this temperature and that bulk pinning has become significant. Equally, the flux profiles show clear evidence of a critical state. Profiles obtained in decreasing field are omitted from Fig. 2(b) for clarity, but are inverted with respect to those in increasing field consistent with bulk pinning and a critical state. At low fields the profiles display a "double dome" which is very similar to the expected profiles predicted for a combination of weak bulk pinning operating together with a surface or geometrical barrier [18].

Figure 2(c) shows local magnetization data in region (C) at 3.60 K. Remarkably, the magnetization loops and field profiles are again like those in Fig. 2(a), displaying asymmetry associated with the surface barrier. This means that bulk pinning has effectively *weakened* with decreasing temperature below T_{AF}^m and hysteresis is again dominated by surface barrier effects.

In order to differentiate more precisely between surface and bulk current flow we determine the gradient of the internal field, dB_z/dx, as described in Ref. [15]. We approximate dB_z/dx as the difference between local field measured at the sample center (sensor 7) and left hand edge (sensor 4) divided by their spatial separation (60 μm). dB_z/dx is then a measure of the net surface or bulk current flow, related to the field gradient, by the Maxwell equations. This construction is illustrated in Figs. 3(a) and 3(b), where we present dB_z/dx for the field profiles shown in Figs. 2(a) and 2(b) where we believe surface barriers and bulk pinning, respectively, to be dominant. In Fig. 3(a) dB_z/dx is always positive and traces out a "clockwise" loop, consistent with surface barriers controlling the hysteretic response [15]. Figure 3(b), on the other hand, shows the opposite, with an "anti-clockwise" loop with equal and opposite magnitudes for ascending and
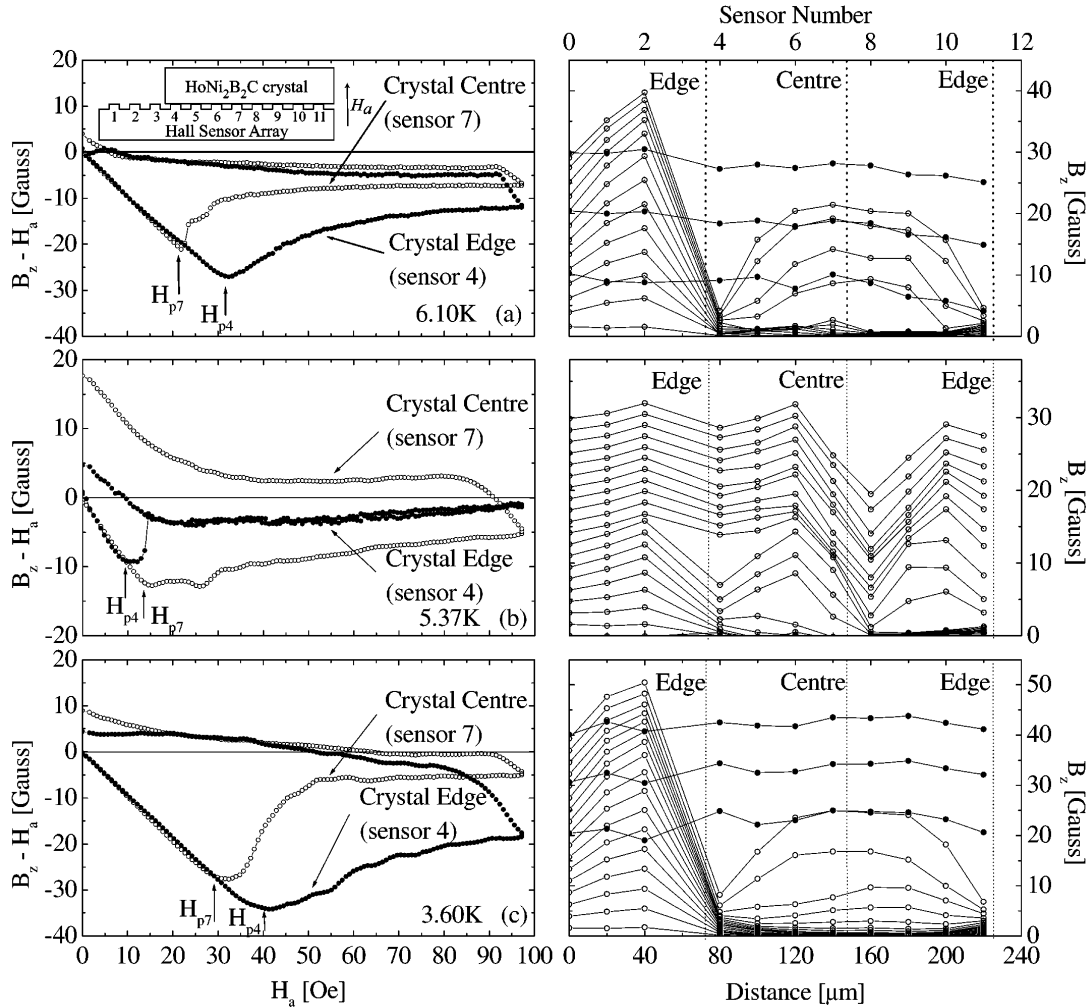
FIG. 2. (Left panel) Local magnetization, $B_z - H_a$ vs H_a, for sensors positioned at the center (7) and edge (4) of a platelet HoNi$_2$B$_2$C crystal at temperatures of (a) 6.10 K, (b) 5.37 K, and (c) 3.60 K. (Right panel) Field profiles measured directly for increasing (open symbols) and decreasing (closed symbols) applied field. The field value indicated at sensor zero represents the external applied field, H_a.

descending field cycles [15]. An estimate for the critical current density can be made directly from the field profiles in Fig. 2(b) and is of the order of 10^3 A/cm^2, confirming that bulk pinning is weak when it appears.

Finally, in Fig. 3(c) we use the above analysis of the field gradients to identify the temperature regimes in which surface and bulk pinning effects dominate the vortex behavior. Figure 3(c) presents dB_z/dx as a function of temperature at a constant applied field of 50 Oe (greater than the full penetration field for the temperature range investigated). Figure 3(a) indicates that dB_z/dx should be positive in increasing field and close to zero in decreasing field when surface barriers dominate the vortex behavior. In the case of bulk pinning effects being dominant, Fig. 3(b) indicates that dB_z/dx is negative in increasing field and positive and of similar magnitude in decreasing field. Figure 3(c) shows a clear crossover between these two behaviors in a narrow temperature range between about 5.1 and 5.75 K, close to

the commensurate and a-axis incommensurate magnetic ordering temperatures T_{AF}^m and T_{ac}^m, respectively.

Inspection of Fig. 1 shows that B_{c2} is suppressed by a factor of about 2 within the temperature range where we observe pinning effects. It is also likely that B_{c1} is suppressed in this temperature regime, as suggested by the variation of the penetration fields marked in Fig. 2(a)–2c, despite the observed pinning effects which can only serve to increase H_p. Surface or geometrical barriers are usually expected to extend to B_c or B_{c1} respectively [16,18] and therefore should be "renormalized" by the suppressed superconducting parameters in this temperature range. This might allow any weak residual pinning effects to be observed which would otherwise be masked by the strong surface or geometrical barrier effects. However, while the overall magnitude of the hysteresis loops decreases in this temperature regime, the increased symmetry of the loops results in a much larger remanent moment than for those measured at either side of this temperature regime where
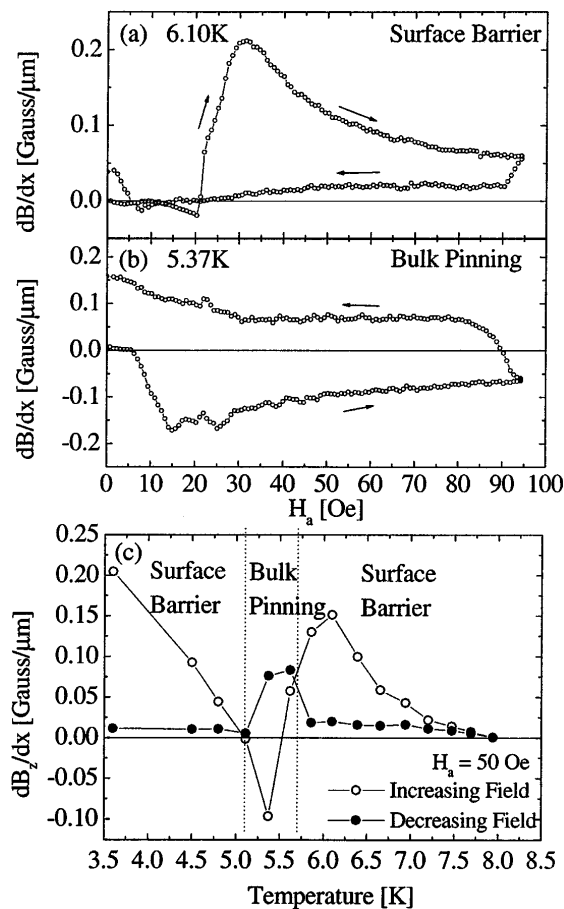
FIG. 3. (a), (b): dB_z/dx vs H_a for the profiles shown in Figs. 2(a) and 2(b). "Clockwise" ("anticlockwise") direction of the loop is due to surface barriers (bulk pinning). (c) dB_z/dx vs temperature for increasing and decreasing field cycles at $H_a = 50$ Oe. Surface barriers dominate the vortex behavior at either side of a "pinning window" between about 5.1 and 5.75 K.

superconductivity is stronger. Furthermore, since the surface barrier does not act to prevent flux exit on decreasing field, it therefore cannot affect the measured flux profiles in this case. Thus, the fact that we observe a significant positive value for dB_z/dx demonstrates unambiguously that pinning has actually *increased* in this temperature regime, regardless of the "strength" of the surface barrier, and is unlikely to arise from any residual material disorder. We therefore propose that the VL in HoNi$_2$B$_2$C for $B \| c$ is pinned at these temperatures due either to interactions with the local Ho moments that lie within the ab plane, or to the modulated magnetic structures. In all regions [(A), (B), and (C)], commensurate or incommensurate AF ordered structures exist in the c- and a-axis directions. The periodicity of the c-axis modulations is equal to the c-axis lattice parameter ($\simeq 10$ Å), or around 130 Å, for the commensurate and

incommensurate structures, respectively, and around 25 Å for the a-axis modulation [5–7]. Since magnetic pinning interactions operate over length scales comparable with the superconducting penetration depth ($\simeq 500$–1000 Å) these modulations should not interact significantly with the VL. On the other hand, the main property of region (B) that is absent in (A) and (C) is the appearance of the a-axis magnetic structure. Since it is magnetic scattering that suppresses B_{c2}, we cannot rule out that there is a corresponding periodic modulation of the coherence length ($\xi_0 \simeq 100$–200 Å) which may lead to a core pinning of vortices. The tetragonal crystal symmetry of HoNi$_2$B$_2$C also means that the a-axis magnetic structure will be broken into "domains" with perpendicular spiral modulations along the two a-axes. These domains may also present significant pinning for vortices by interaction with the domain walls. Both scenarios are consistent with our observations of enhanced pinning effects coinciding only with the occurrence of the a-axis modulated magnetic structure in region (B).

In summary, we have used a miniature local Hall array to investigate the flux profiles in single crystals of the magnetic superconductor HoNi$_2$B$_2$C. Surface barriers dominate the behavior at high temperatures (6 K to T_c) and below $T_{AF}^m \simeq 5$ K. Bulk pinning only becomes important between these temperatures (5 to 5.75 K), coinciding with the appearance of the a-axis incommensurate magnetic spiral state and the strong suppression of B_{c2}. We propose that pair breaking cannot entirely account for the enhanced pinning observed here, and suggest a direct interaction between the vortex lattice and a-axis ordered magnetic states, or domains thereof, leads to a pinning of vortices.

[1] R. Nagarajan *et al.,* Phys. Rev. Lett. **72**, 274 (1994).
[2] R. J. Cava *et al.,* Nature (London) **367**, 148 (1994).
[3] P. C. Canfield *et al.,* Physica (Amsterdam) **230C**, 397 (1994).
[4] H. Eisaki *et al.,* Phys. Rev. B **50**, 647 (1994).
[5] A. I. Goldman *et al.,* Phys. Rev. B **50**, 9668 (1994).
[6] K. H. Müller *et al.,* J. Appl. Phys. **81**, 4240 (1997).
[7] L. J. Chang *et al.,* Phys. Rev. B **54**, 9031 (1996).
[8] V. G. Kogan *et al.,* Phys. Rev. B **55**, R8693 (1997).
[9] U. Yaron *et al.,* Nature (London) **382**, 236 (1996).
[10] M. R. Eskildsen *et al.,* Phys. Rev. Lett. **79**, 487 (1997).
[11] D. McK. Paul *et al.,* Phys. Rev. Lett. **80**, 1517 (1998).
[12] M. R. Eskildsen *et al.,* Nature (London) **393**, 242 (1998).
[13] K. Krug *et al.,* Physica (Amsterdam) **267C**, 321 (1996).
[14] M. Xu *et al.,* Physica (Amsterdam) **227C**, 321 (1994).
[15] E. Zeldov *et al.,* Europhys. Lett. **30**, 367 (1995).
[16] C. P. Bean *et al.,* Phys. Rev. Lett. **12**, 14 (1964).
[17] M. Konczykowski *et al.,* Physica (Amsterdam) **194C**, 155 (1992).
[18] E. Zeldov *et al.,* Phys. Rev. Lett. **73**, 1428 (1994).